Development of Kinetic and Process Model for Oxidative Desulphurization of Light Fuel using Experiments and Parameter Estimation Technique

Amer T. Nawaf[1], Aysar T. Jarullah [1,2], Saba A. Gheni [1],
Iqbal M. Mujtaba[3,4]

[1]Chemical Engineering Department, College of Engineering, Tikrit University

[2] Email: A.T.Jarullah@tu.edu.iq

[3]Chemical & Process Engineering Division, University of Bradford, Bradford BD7 1DP, UK

[4] Email: I.M.Mujtaba@bradford.ac.uk

Abstract

The oxidative desulphurization (ODS) of light gas oil (LGO) is investigated with an in-house designed cobalt oxide loaded on alumina (γ-Al_2O_3) catalyst in the presence of air as oxidizing agent under moderate operating conditions (temperature from 403 to 473 K, LHSV from 1 to 3 hr^{-1}, initial concentration from 500 to 1000 ppm). Incipient Wetness Impregnation method (**IWI**) of cobalt oxide over gamma alumina (2% Co_3O_4/γ-Al_2O_3) is used for the preparation of the catalyst. The optimal design of experiments is studied to evaluate the effects of a number of process variables namely temperature, liquid hourly space velocity (LHSV) and concentration of dibenzothiophene and their optimal values were found to be 473 K, 1hr^{-1} and 1000 ppm respectively. For conversion dibenzothiophene to sulphone and sulphoxide, the results indicates that the Incipient Wetness Impregnation (**IWI**) is suitable to prepare this type of the catalyst. Based on the experiments, mathematical models that represent a three phase reactor for describing the behavior of the ODS process are developed.

In order to develop a useful model for simulation, control, design and scale-up of the oxidation process, accurate evaluation of important process parameters such as reaction rate parameters is absolutely essential. For this purpose, the parameter estimation technique available in gPROMS (general Process Modelling System) software is employed in this work. With the estimated process parameters further simulations of the process is carried out and the concentration profiles of dibenzothiophene within the reactor are generated.

Key words: ODS, Trickle bed reactor, Mathematical model, Kinetic parameter technique

1. Introduction

Sulphur compounds (mainly, benzothiophene (BT), dibenzothiophene (DBT) and its derivatives) in oil (fuels) are the main source of air pollution, due to generation of sulphuroxides by the combustion process leading to acid rain. The traditional mode of removal of sulphur in fuels is by catalytic hydrodesulphurization (HDS), commonly known as hydrotreating, and requires modified catalyst and severe operating conditions (temperature, pressure, etc.). This make the hydrotreating process more expensive compared to other processes[1-3]. Thiophene compound and its aromatic compounds are the main sulphur components found in the oil feedstock. Sulphur decreasing in the fuel has gained significance owing to increasing awareness about the serious consequences of burning sulphur-bearing fuels. The U.S. Environmental Protection Agency (EPA) had constituted new sulphur standers of diesel fuels and gasoline.[1]

Oxidative desulphurization (ODS) process is regarded as one of the most promising alternative deep desulphurization operations to get ultra-low sulphur fuels. [1,4,5] The ODS process of sulphur compounds such as, thiophene (Th), benzothiophene (BT), dibenzothiophene (DBT) and their compounds are investigated by employing various solid catalysts like Mo-Al_2O_3[6,7]Cobalt–aluminium phosphate[8], where the sulphur components are oxidized into their corresponding sulfoxides and sulphones. The greatest advantage of ODS in comparison to HDS process is that the ODS can be conducted in a liquid phase under moderate conditions. In Oxidative desulphurization reactions, the sulphur compound is oxidized via adding oxygen molecules to form the hexavalent sulphur of sulphones.[9]

The idea of ODS is actually quite simple. Sulphur compounds are known to be slightly more polar than hydrocarbons of similar structure[10,11]. However, oxidized sulphur compounds such as sulphones or sulfoxides are substantially more polar than unoxidised sulphur compounds. This permits the selective removal of sulphur compounds from hydrocarbon by a combination process of selective oxidation and solvent extraction or solid adsorption[12]. Before 1980, the most popular oxidants in the study of ODS are nitric acid and nitrogen oxides and used largely because they have double effects of oxidizing sulphur compounds and nitrating the aromatic compounds to form nitro aromatics with high cetane numbers. However, it has major drawbacks such as poor selectivity, low yield and loss of heating value of the treated oil[12,13]. Other types of oxidants have also been used, including H_2O_2/AcOH, H_2O_2/H_2SO4, O_3, $KMnO_4$ and BuOOH[14,15,16],oxygen[17] and O_2/aldehyde/cobalt catalysts [18].

Three phase reactors with fixed bed of catalyst and co-current down flow of gas and liquid, are utilized widely in different oil, petrochemical and chemical industries besides water industries treating wastewater. Understanding the phenomena that govern the performance of three-phase reactors has played a significant role in designing of such equipment. The hydrodynamic factors such as pressure drop, liquid hold up and catalyst wetting efficiency together with characterization of reaction kinetics as well as transport in catalyst particles are all-important and should to be considered for developing an accurate model of the process. Plug flow model for the liquid phase with modified external liquid holdup, external contacting catalyst effectiveness parameters have been suggested by several investigators in the past.[9,20]

Based on experimental studies with an in-house designed catalyst, the aim of this study is to develop kinetic models for the ODS process. For this purpose, a full process model available in the public domain is used and the reaction parameters of the model are determined by minimizing (optimization) sum of the squared error between the data obtained experimentally and those predicted by the model. The modeling, simulation and optimization process of ODS operation are carried out employing gPROMS software.[21]

2. Experimental Work

2.1 Feedstock (Light Gas Oil)

Light gas oil (LGO), the feedstock used in this study, is provided by the North Refineries (Iraq) with the following specifications: 0.851 sp.gr, 4.9 cSt viscosity at 293K, 55^{o}C flash point, 9.8 ppm total sulphur, 52 cetane index and -39^{o}C pour point, which are tested in North Refineries Company laboratories.

2.2 Dibenzothiophene (DBT)

The dibenzothiophene (DBT) obtained from Aldrich is chosen to study the reactivity of sulphur in the oxidation reaction. Purity of sulphur compound is about 98%.

2.3 Air

Air gas is used as oxidant agent. Oxygen contained in air can be oxidant to sulphur compounds.

2.4 Catalyst

Chemical compounds are used for catalyst preparation, as follow:

2.4.1 Active compound used in the catalyst preparation

Specifications of the active compound used in the catalyst preparation are shown in Table 1 below.

Table 1: List of chemicals and materials used for catalyst preparation and Aluminum oxide specifications

Chemicals and Materials	**Purity%**	**Function**	**Manufacture**
Cobalt nitrate $Co(NO_3)_2.6H_2O$	99.5	Active material	Alpha chemica
Deionized water	-	Solvent of active material	Samarra company

Aluminum oxide(γ-Al_2O_3) specifications

Catalyst	Pore volume (cm^3/g)	Bulk density (g/cm^3)	Surface area (m^2/g)	Particle diameter (mm)	Particle shape
γ-Al_2O_3	0.5367	0.671	289	1.6	Sphere

2.4.2 Supported alumina oxide (γ-Al_2O_3)

The specification of a commercial spherical particle alumina oxide -type gamma alumina (γ) is also presented in Table 1, which has been used as a carrier in the manufacturing of catalyst.

2.5 Catalyst Preparation used in Experimental Work

The cobalt solution (Cobalt nitrate) supported on alumina (γ-Al_2O_3) has been obtained by **IWI** method. The preparation procedure is as follows: firstly, 100 gm of the alumina dries in the furnace at 393K for 4 hour for removing the moisture from alumina before impregnation. Secondly, 2.1 gm of cobalt nitrate is added to 40 cm^3 deionized water (pore volume of gamma alumina equal to deionized water volume), while the solution is being stirred (using magnetic stirrer) for one hour at room temperature. The pretreated gamma alumina in step one is then transferred into a flask under vacuum (utilizing vacuum pump) for removing gases out of support pores. After that, the solution obtained in the second step is added to gamma alumina with 15-20 drop/min rating and continuous stirring until impregnation of all the solution is complete. The temperature is kept constant at 373 K using a bath water. The impregnated gamma alumina is then left to dry overnight in the furnace at 393K. The aim of this step is to eliminate water. The calcination step is then applied for five

hours in the furnace at 823 K with air. This step converts the metal salts deposited on the γ-Al_2O_3 into metal oxides allowing deposition of active metal oxides on the catalyst support and thus desired physical and chemical specifications of the catalyst are achieved. Calcination step is conducted in ***Fertilizer/Northern Company*- Baiji**. Figure 1 illustrates the steps and sequence of activities in the catalyst preparation

2.6 Oxidation Operation in Trickle Bed Reactor

2.6.1 Apparatus and Procedure

The experiments are carried out at high temperature and pressure in a trickle bed reactor (TBR) reactor available in Tikrit University (Iraq). TBRs are extensively utilized in oil refineries and the process flow diagram of this system is presented in Figure 2. Three phases existing in such systems are: solid phase (catalyst bed), gas phase (air) and liquid phase (LGO). The continuous oxidation of LGO is carried out in the TBR where the LGO and air are fed in co-current mode. The reactor is made of stainless steel with inside diameter of 1.6 cm and length of 77 cm. Four steel-jacket heaters of equal length are used to control the reactor temperature. The top and bottom (30 to 35 % by volume at each end) parts of the reactor are filled with inert particles to serve as disengaging part. The inner part (40% vol.) of the reactor contains a packing of cobalt oxide catalyst.[22]The LGO is pumped at pressure up to 20 bar with flow rates from 0.0 to 1.65 l/hr. The oxidant gas (air) flows from an air compressor at high pressure and fixed operation pressure is maintained. The LGO with varying DBT concentration is mixed with air before feeding into to the reactor at the desired temperature allowing DBT to oxidize to sulphones. The outlet from the reactor flows through a heat exchanger to high-pressure gas-liquid separator in order to separate excess air from the treated LGO. The description and specifications of the experimental equipment can be found in Nawaf et al.[38]

2.6.2 Experimental Runs

The effect of operational parameters on the reactor performance of ODS using cobalt oxide (Co_3O_4/γ-Al_2O_3) catalyst is evaluated by varying temperature between 403 and 473K and liquid hourly space velocity (LHSV) between 1 - 3 hr^{-1}. The concentration of dibenzothiophene is varied between 500 and 1000 ppm. The oxidation experiments have been conducted in a trickle bed reactor packed with 40% catalyst particles at isothermal condition. The model light gas oil is prepared by adding of DBT to hydro-treated light gas oil (containing 2 ppm of DBT)with specified initial concentrations of DBT. The temperature of the LGO feed tank is controlled using a cooling jacket where the coolant side temperature is maintained below 293K for preventing vaporization of light compounds found in light gas oil. To prevent leaks and to remove any gases

and liquid remained from the last run Nitrogen gas is passed through the reactor.LGO mixed with air is then passed through the reactor at 2-bar pressure and temperature controller is set to the desired feed temperature. When the air temperature reaches feed injection temperature the dosing pump is turned on to allow a certain light gas oil flow rate and the temperature is raised at the rate of 293K per hour until steady state temperature is reached. At the end of a run, the LGO dosing pump is turned off keeping air gas flow on to backwash any remaining light gas oil. Finally, the air valve is shutoff.

2.6.3 Sulphur Measurements (GC-capillary Chromatography)

Dibenzothiophene concentration in feed and product are evaluated according to GC-capillary chromatography. The detailed specifications of the GC-capillary chromatography is given in Naefet al.[38]

3. Mathematical Model of TBR for ODS Reaction

Process model plays a very important role in industries from operator training, health and safety to design, operation and control. [23]Several investigators have suggested that pore diffusion should be considered within the reaction rate constant (multiplying intrinsic rate constant by effectiveness factor) resulting in a pseudo homogeneous basic plug flow model which is adequate for describing the progress of chemical reactions in the liquid phase of a trickle bed reactor. [20,24,25]

3.1 Mass Balance Equations

Figure 3 shows a typical TBR with various features (assumption, operation parameters, software used, etc.). The general mass balance for a reactor can be described as:

[Mass In] = [Mass Out] + [Mass Disappearance/Appearance by chemical reaction] + [Accumulation] (1)

Input of DBT, moles / time = F_{DBT}, Output of DBT moles / time = $F_{DBT} + dF_{DBT}$, Disappearance of DBT by reaction moles / time = $(-r_{DBT})dV$, Accumulation of dibenzothiophene = 0

$$F_{DBT} = (F_{DBT} + dF_{DBT}) + (-r_{DBT})dV \quad (2)$$

$$dF_{DBT} = d[\, F_{DBT0}(1-X_{DBT})\,] = -\, F_{DBT0}dX_{DBT} \quad (3)$$

Since $F_{DBT} = C_{DBT}v_L$, Where C_{DBT} concentration of dibenzothiophene, moles / volume

v_L is the volumetric flow rate, volume /time, We obtain on replacement:

$$F_{DBT0}\, dX_{DBT} = (-r_{DBT})dV \quad (4)$$

The equation above accounts for DBT compound in the differential part of catalyst vol. (dV). For the catalytic reactor as a whole, the term should be integrated. Now F_{DBT0}, the feed rate, is fixed, but $(-r_{DBT})$ certainly depends on the concentration or conversion of materials.

$$\tau = C_{DBT0} \int_0^{X_{DBTf}} \frac{dX_{DBT}}{-r_{DBT}} \quad (5)$$

3.2 Chemical Reaction Rate

Kinetic models are essential for catalyst testing at laboratory scale and for comparing various catalysts for a given task such as ODS. Amongst various methods, parameter estimation technique is one of them where a kinetic model is assumed but its parameters are adjusted by comparing the model predictions with the experimental observations.[26] To appreciate the complexity of the chemical reaction one should start with an *n-th* order kinetics:

$$-r_{DBT} = -\frac{dC_{DBT}}{dt} = K_{app} C_{DBT}^{n} \quad (6)$$

Apparent kinetics are relating with the intrinsic kinetics regarding internal diffusion and trickle bed reactor hydrodynamic influences as follows: [27]

$$K_{app} = \eta_0 \eta_{ce} K_{in} \quad (7)$$

Where, internal diffusion is described by the catalyst effectiveness factor (η_0) and the hydrodynamics by the external catalyst wetting efficiency (η_{ce}). The chemical reaction is produced as:

$$-r_{DBT} = -\frac{dc_{DBT}}{dt} = K_{in} \eta_0 \eta_{ce} C_{DBT}^{n} \quad (8)$$

Reaction rate constant for ODS reaction (K_{in}) can be estimated for each reaction utilizing the Arrhenius equation as follows:

$$K_{in} = K_0 \, e^{-\frac{EA}{RT}} \quad (9)$$

K_0 is the frequency or pre-exponential factor and (EA) is the activation energy of the reaction. This term fits experiment well over wide temperature ranges and is highly proposed from different standpoints as being a very good approximation to the actual temperature dependency. The chemical reaction rate can be expressed as:

$$-r_{DBT} = -\frac{dc_{DBT}}{dt} = K_0 e^{-\frac{EA}{RT}} \eta_0 \eta_{ce} C_{DBT}^{n} \quad (10)$$

If the catalytic reaction of dibenzothiophene oxidation obey n^{th}-order kinetic can be integrated and get final expression:

$$\frac{1}{n-1}\left[\frac{1}{C_{DBTf}^{n-1}} - \frac{1}{C_{DBT0}^{n-1}}\right] = \frac{k_{app}}{LHSV} \quad (11)$$

3.3 Reactor Description

The TBR includes a number of control variables: mass transfer coefficients, viscosity and density of the oil, diffusivities, effectiveness factor and others. These factors are evaluated utilizing the relations presented in the literatures as follows. For accounting into hydrodynamics and other physical impacts, an apparent kinetic constant can be stated: $K_{app} = K_{in}.f$ (hydrodynamics) and is rewritten as (note that $\eta_0\eta_{ce}K_{in}$ is employed instead of K_{app}):

$$\frac{1}{n-1}\left[\frac{1}{C_{DBTf}^{n-1}} - \frac{1}{C_{DBT0}^{n-1}}\right] = \frac{\eta_0\eta_{ce}K_{in}}{LHSV} \quad (12)$$

The effectiveness factor (η_0) is to be calculated as function of Thiele modulus (Φ) with the following correlations employed for sphere particles: [28]

$$\eta_0 = \frac{3(\Phi\coth\Phi - 1)}{\Phi^2} \quad (13)$$

Generally, Thiele modulus (Φ) for nth-order irreversible reaction is as follows: [24]

$$\Phi = \frac{V_P}{S_P}\sqrt{\left(\left(\frac{n+1}{2}\right)\frac{K_{in}(C_{DBT})^{n-1}\rho_p}{D_{ei}}\right)} \quad (14)$$

$$\rho_p = \frac{\rho_B}{1-\epsilon_B} \quad (15)$$

The effective diffusivity (D_{ei}), where the structure (porosity and tortuosity) of the pore network inside the particle is taken into account through the modeling. [29]

$$D_{ei} = \frac{\epsilon_S}{\mathcal{T}}\frac{1}{\frac{1}{D_{mi}}+\frac{1}{D_{ki}}} \quad (16)$$

Catalyst porosity (ϵ_S) can be estimated with the following relation based on experiments of total pore volume (V_g):

$$\epsilon_S = \rho_p V_g \quad (17)$$

The effective diffusivity depends on Knudsen diffusivity D_{ki} and molecular diffusivityD_{mi}whichcan be evaluated as follows: [32 ,31 ,30]

$$D_{ki} = 9700\, r_g \left(\frac{T}{MW_i}\right)^{0.5} \quad (18)$$

Tyn-Calus correlation:

$$D_{mi} = 8.93 \times 10^{-8} \frac{v_L^{0.267} T}{v_{DBT}^{0.433} \mu_L} \quad (19)$$

The molar volume of light gas oil (L), can be calculated by the following equation:

$$v_{DBT} = 0.285(v_{cDBT})^{1.048} \quad (20)$$

The critical specific volume of light gas oil (liquid) can be evaluated by a **Riazi–Daubert** equation: [33]

$$V_L = 0.285(v_{cL})^{1.048} \quad (21)$$

$$v_{cL} = (7.5214 \times 10^{-3}(T_{meABP})^{0.2896}(\rho_{15.6})^{-0.7666}) MW_L \quad (22)$$

Mean pore radius [20]:

$$r_g = \frac{2V_g}{S_g} \quad (23)$$

The tortuosity factor ($\mathcal{T}$) of the pore structure,in equation (16) is given by:[30]

$$\frac{1}{\mathcal{T}} = \frac{\epsilon_S}{1 - \frac{1}{2}\log(\epsilon_S)} \quad (24)$$

The external catalyst wetting efficiency of the surface η_{ce}, is determined at atmosphere pressure utilizing the equation of **Al-Dahhanand Dudukovic.** [34]

$$\eta_{ce} = 1.617 Re_L^{0.146} Ga_L^{-0.071} \quad (25)$$

Reynolds number:

$$Re_L = \frac{\rho_L u_L d_p}{\mu_L} \quad (26)$$

Modified Reynolds number is introduced as:

$$Re_L^{''} = \frac{\rho_L u_L d_p}{\mu_L (1-\epsilon_B)} \quad (27)$$

Galileo number:

$$Ga_L = \frac{d_p^3 \rho_L^2 g}{\mu_L^2} \quad (28)$$

Modified Galileo number:

$$Ga_L^{''} = \frac{d_p^3 \rho_L^2 g \epsilon_B^3}{\mu_L^2 (1-\epsilon_B)^3} \quad (29)$$

Bed porosity (bed void fraction) for undiluted catalyst bed may be evaluated utilizing the equations reported by **Froment and Bischoff,**[28] and introduced by **Jarullah et al.:** [35]

$$\epsilon_B = 0.38 + 0.073 \left(1 + \frac{\left(\frac{d_t}{d_{pe}} - 2\right)^2}{\left(\frac{d_t}{d_{pe}}\right)^2}\right) \quad (30)$$

ϵ_B Catalyst bed porosity, equivalent particle diameter (d_{pe}), defined as the diameter of a sphere that has the same external surface (or volume) as the actual catalyst particle, which is a sufficient particle characteristic depending upon the particle shape and size.

$$d_{pe} = d_p = 1.6\ mm \quad (31)$$

Where (V_P) external volume and (S_P) catalyst surface. The external volume and surface of regular shape (spherical) can be estimated as:

$$V_P = \frac{4}{3}\pi\left(r_p\right)^3 \quad (32)$$

$$S_P = 4\pi\left(r_p\right)^2 \quad (33)$$

The LGO density (ρ_L) as a function of process conditions is calculated by the **Standing-Katz** correlation: [20]

$$\rho_L = \rho_o + \Delta\rho_p - \Delta\rho_T \quad (34)$$

$$\Delta\rho_p = (0.167 + 16.181 \times 10^{-0.0425\rho_0}).\left(\frac{P}{1000}\right) - 0.01 \times (0.299 + 263 \times 10^{-0.0603\rho_0}).\left(\frac{P}{1000}\right)^2 \quad (35)$$

The temperature employed for equation of the liquid density in this relation:

$$\Delta\rho_T = (0.0133 + 152.4(\rho_o + \Delta\rho_P)^{-2.45}).(T - 520) - \left(8.1 \times 10^{-6} - 0.0622 \times 10^{-0.764(\rho_0 + \Delta\rho_P)}\right).$$

$$(T - 520)^2 \quad (36)$$

Glaso's correlation has utilized as a generalized correlation for oil viscosity, as follows: [36]

$$\mu_L = 3.141 \times 10^{10}(T - 460)^{-3.444}[\log_{10} API]^a \quad (37)$$

$$a = 10.313[\log_{10}(T - 460)] - 36.447 \quad (38)$$

The (API) is shown in this equation:

$$API = \frac{141.5}{Sp.gr_{15.6}} - 131.5 \quad (39)$$

The set of equations from 1 to 39 were coded and solved simultaneously using the gPROMS. [21]

4. Parameter Estimation Techniques

Accurate determination of process parameters is essential to benefit from any model-based activities such as design, control, scale-up, etc.[32, 37] Evaluation of reaction rate parameters can be accomplished via parameter estimation technique based on experimental data and model predictions so that errors between experimental and predicted data are minimized. The experimental data of the ODS process considered in this work were matched against a simple power law kinetic model (equation 8):

$$-r_{DBT} = -\frac{dc_{DBT}}{dt} = K_{in}\eta_0\eta_{ce}C_{DBT}^{n}$$

Calculated yields have estimated by integration of equation 8, where $\mathbf{C_{DBT0}}$ is the feed concentration of DBT:

$$C_{DBTf}^{calc.} = \left(\frac{C_{DBT0}^{n-1}\times LHSV}{C_{DBT0}^{n-1}\eta_0\times\eta_{ce}\times K_{in}\times(n-1)+LHSV}\right)^{1/(n-1)} \quad (40)$$

Where, C_{DBTf} product concentration of DBT, LHSV and n the reaction order. For parameter estimation, the objective function, ***OBJ***, as presented below, has minimized:

$$OBJ = \sum_{n=1}^{N_t}\left(C_{DBT}^{meas.} - C_{DBT}^{prid.}\right)^2 \quad (41)$$

In Eq. (41), N_t,$C_{DBT}^{meas.}$ and $C_{DBT}^{prid.}$ are the numbers of test runs, the evaluated product yield and the predicted one by model, respectively. Using the kinetic parameters reported in the literature (without optimization), the composition of all fractions was estimated via application of model correlations in gPROMS. The comparison between experimental and predicted results using the kinetic parameters published in the literature (without the optimization) is listed in Table 2. As shown in this Table, there is a big variation between estimated and experimental values; therefore, optimization is employed on model variables for minimizing this variation.

4.1 Optimization Problem Formulation for Parameter Evaluation

The parameter evaluation problem formulation is described as follows:

Given The reactor configuration, the catalyst, the feedstock, the operation conditions

Optimize The reaction orders of ODS (n_1), reaction constants (k) at various temperatures (403, 443, 473, respectively).

So as to minimize The sum of squared errors (*OBJ*).

Subject to Constraints on the conversion and linear bounds on all optimization variables

Mathematically, the problem is stated as:

Min. OBJ

$n^j, k_i^j,$ $(i=1\text{-}3, j=Co_3O_4/\gamma\text{-}Al_2O_3)$

S.t. $\mathbf{f(z, x(z), \underline{x}(z), u(z), v) = 0}$

$$(C_L \le C \le C_U)$$

$$(n^j_L \le n^j \le n^j_U)$$

$$(k_i^j{}_L \le k_i^j \le k_i^j{}_U)$$

Table 2: Model prediction with parameters from the literature and experimental data (DBT, $Co_3O_4/\gamma\text{-}Al_2O_3$)

I.C (ppm)	LHSV (hr^{-1})	Temperature (K)	Predicted	Experimental	Error%
1000	1	403	822.177	701.760	17.159
1000	1	443	717.156	460.640	55.686
1000	1	473	503.349	220.000	128.79
800	1	403	678.446	586.809	15.616
800	1	443	603.245	410.598	46.918
800	1	473	441.429	199.546	46.918
500	1	403	446.277	379.577	17.572
500	1	443	410.243	272.823	50.369
500	1	473	324.457	153.926	110.78
1000	2	403	893.842	760.230	17.575
1000	2	443	822.824	614.968	33.799
1000	2	473	653.279	408.000	60.117
800	2	403	728.239	634.657	14.745
800	2	443	678.879	510.600	32.995
800	2	473	556.037	352.270	57.843
500	2	403	468.904	407.661	15.023
500	2	443	446.371	342.989	30.141
500	2	473	386.328	236.946	63.304
1000	3	403	922.842	877.190	5.2040
1000	3	443	868.632	722.470	20.230
1000	3	473	729.749	501.790	45.429
800	3	403	750.813	717.110	4.6990
800	3	443	715.329	635.286	12.599
800	3	473	620.541	450.436	37.764
500	3	403	447.672	458.840	2.4330
500	3	443	461.011	414.986	11.091
500	3	473	414.483	289.723	43.062

Where, $\mathbf{f(z, x(z), \underline{x}(z), u(z), v) = 0}$ refers to the mathematical model of the process, **z** denotes the independent variable, **u(z)** is the optimization variable, **x(z)** is the set of all differential and algebraic variables, $\underline{\mathbf{x}}\mathbf{(z)}$ represents the derivatives of differential variables with respect to **z**, and **v** refers the fixed parameters. **C** is the concentration and C_L, C_U are the lower and upper bounds of concentration. **L** and **U** denote the bounds of the parameters concerned.

The optimization solution method utilized by gPROMS is a two-step way known as feasible path approach described in detail in Nawaf et al.[38] and Jarullah et al.[29,32,35]. The values of constant factors employed in the models are listed in Table 3. Note, to avoid local minima, the solutions are checked by starting with different initial guesses of the parameters. In gPROMS, one can also provide default (initial) values of the parameters with wide bounds (lower and upper bounds).

Table 3: Values of constant factors utilized in the ODS models

Factors	Symbol	Unit	Value
Initial concentration	C1, C2, C3	wt	C1=0.1, C2= 0.08, C3= 0.05
Temp.	T1, T2, T3,	K	T1= 403, T2= 443, T3= 473
Liquid hourly space velocity	LHSV1, LHSV2, LHSV3	hr^{-1}	LHSV1=1, LHSV2= 2, LHSV3= 3
Press.	P	Psia	14.7
Density of LGO at 15.6 ^{o}C and 101.3 kPa	Den_0	Ib/ft^3	52.58307119
Gas constant	R	J/mole. K	8.314
Volume of catalyst particle	V_p	cm^3	0.00214
Total geometric external area of particle	S_p	cm^2	0.0804
Bulk density	$\rho_{B\,Co}$	g/cm^3	$\rho_{B\,Co} = 0.692$
pore volume per unit mass of catalyst	V_g	cm^3/g	$V_{g\,CO} = 0.5021$
M.w of O_2	MW_i	g/gmole	0.21
M.w of LGO	MW_L	g/gmole	212.12
Critical specific volume of the DBT compound	V_{CDBT}	ft^3/mole	8.2176
Mean average boiling point	T_{meABP}	R	981.27
Specific surface area of particle	S_g	cm^2/g	S_{gCO}= 2500000
Tube diameter	d_t	cm	1.6
Velocity of light gas oil	u_{L1}, u_{L2}, u_{L3}	cm/sec	u_{L1}=0.00799, u_{L2}= 0.01599, u_{L3}= 0.02368
Acceleration gravity	g	cm/sec^2	981

5. Results and Discussions

5.1 Experimental Results

Effect of Catalyst Loading on Process Conversion at Operating Conditions

The influence of initial concentration, reaction temperature, LHSV and catalyst loading on the process conversion is investigated. Below 403 K, high conversion has not been observed on the processes. No apparent difference in conversion for the oxidation of model light gas oil catalyzed by temperature of 403 K and LHSV of $3hr^{-1}$ was noticed. The optimal results were obtained with a temperature of 473 K, LHSV of 1 hr^{-1} and initial concentration of 1000 ppm. The results of experimental runs are shown in Table 4.

Table 4: Experimental results obtained from process conditions

I.C (ppm)	Temp. (K)	LHSV(hr^{-1})	Outlet concentration (ppm)	Conversion
1000	403	1	701.760	0.298
1000	403	2	760.230	0.240
1000	403	3	877.190	0.123
1000	443	1	460.640	0.539
1000	443	2	614.968	0.385
1000	443	3	722.470	0.278
1000	473	1	220.000	0.780
1000	473	2	408.000	0.592
1000	473	3	501.790	0.498
800	403	1	586.809	0.267
800	403	2	634.657	0.207
800	403	3	717.110	0.104
800	443	1	410.598	0.487
800	443	2	510.600	0.362
800	443	3	635.286	0.209
800	473	1	199.546	0.751
800	473	2	352.270	0.559
800	473	3	450.436	0.437
500	403	1	379.577	0.241
500	403	2	407.661	0.185
500	403	3	458.840	0.082
500	443	1	272.823	0.454
500	443	2	342.989	0.314
500	443	3	414.986	0.170
500	473	1	153.926	0.692
500	473	2	236.946	0.526
500	473	3	289.723	0.421

The oxidation reactivity of DBT was also investigated at different temperatures (403 – 473 K, and different LHSV (1 – 3 hr^{-1}), in the presence of the (Co_3O_4/γ-Al_2O_3) catalyst. The effects of LHSV and temperature on DBT oxidation are shown in Figure 4a. At low temperature, the oxidative conversion of DBT was very low then increased gradually with increasing reaction temperature from 403 to 473 K and the rate of DBT oxidation increased to 78 % at 473 K, 1 hr^{-1} and 1000 ppm.

The effect of LHSV on DBT removal rate is presented in Figure 4b. It can be seen, increasing LHSV has an adverse impact on DBT conversion. Figure 4b depicts the effect of liquid flow rate on DBT conversion. As clearly noted from this Figure, DBT conversions at 1000 ppm and 473 K is 75.1% obtained at LHSV=1 hr^{-1}. Note, at LHSV of 2 and 3 hr^{-1}, DBT conversions were 55.9 % and 43.7 % respectively.

Actually, rising liquid flow rate will lead to reduce the contact time of the reactant hence decreasing the time of reaction of DBT with air. Moreover, lower LHSV give higher liquid holdup, which evidently decrease the contact of liquid and gas reactants at the catalyst active site, by incrementing film thickness.

The sulphur content has decreased with incrementing sulphur concentration and the reaction temperature. This is due to the fact that with higher sulphur conversion its oxidative ability towards formation of corresponding sulphone derivatives decreases. As shown in Figure 4c, present study agrees to the results published by **Sachdeva and Pant** [39] related to the oxidation of dibenzothiophene.

The obtained kinetic factors generated by optimization process for oxidative desulfurization operation are listed in Table below. The minimization of the objective function depending upon the sum of squared errors between the experimental and estimated results compositions, has applied to obtain the best set of kinetic factors. Optimal model parameters obtained by optimization process show in Table 5:

Table 5: Optimal model parameters obtained by optimization process:

Parameter	Value	Units
n	1.439	(--)
K1	0.499	$(hr^{-1} * (Wt)^{-0.43893})$
K2	1.036	$(hr^{-1} * (Wt)^{-0.43893})$
K3	2.483	$(hr^{-1} * (Wt)^{-0.43893})$

Note that in our previous study (Nawaf et al. [38]), an optimal design of TBR via improving kinetic model depending on the pilot plant experiments using different catalyst (in-house designed manganese oxide (MnO_2/γ-Al_2O_3) catalyst) for the ODS of dibenzothiophene in LGO was discussed in details. It has been observed that the kinetic factors generated here are different compared with those factors obtained in our previous work, which gives a clear indication that the kinetic model for ODS process depends namely upon the kind of the catalyst utilized. The difference between the catalysts used is attributed to their differences in physical and/or chemical properties. Regarding the results of using MnOx/Al_2O_3 and CoOx/Al_2O_3, it seems that the activity of these catalysts is related to the metal dispersion, BET surface area, porosity, and bulk density. The catalysts are ranked as follows in terms of activity in DBT oxidation. Between the two catalysts, the manganese oxide showed a good impregnation (MnO_2=13%), compared to cobalt oxide (2%CO_3O_4).

5.2 Model Validation

The process model developed in this work is simulated further within gPROMS software. The experimental results versus simulation results obtained by the optimization technique are presented in Table 6. A comparison between experimental results and model predictions for ODS of LGO have also shown in Figures 5a, b, c, d, e which demonstrate that the model can simulate the behavior of the TBR very well within the range of operating conditions with average absolute error less than 5% among all the results obtained.

Table 6: Model prediction and experimental results (Dibenzothiophene, $Co_3O_4/\gamma\text{-}Al_2O_3$)

I.C (ppm)	LHSV (hr^{-1})	Temperature (K)	Concentration by Simulation	Conversion by Simulation	Experimental Concentration	Experimental Conversion	Error%
1000	1	403	675.299	0.325	701.760	0.298	3.918
1000	1	443	478.497	0.522	460.640	0.539	3.732
1000	1	473	231.005	0.787	220.000	0.780	4.764
800	1	403	558.699	0.302	586.809	0.267	4.978
800	1	443	405.951	0.493	410.598	0.487	1.145
800	1	473	204.598	0.744	199.546	0.751	2.469
500	1	403	371.655	0.257	379.577	0.241	2.131
500	1	443	283.431	0.433	272.823	0.454	3.743
500	1	473	155.753	0.688	153.926	0.692	1.173
1000	2	403	798.248	0.202	760.230	0.240	4.763
1000	2	443	646.799	0.353	614.968	0.385	4.921
1000	2	473	399.558	0.600	408.000	0.592	2.112
800	2	403	651.447	0.149	634.657	0.207	2.577
800	2	443	536.764	0.263	510.600	0.362	4.874
800	2	473	342.847	0.457	352.270	0.559	2.748
500	2	403	422.327	0.155	407.661	0.185	3.473
500	2	443	359.175	0.282	342.989	0.314	4.506
500	2	473	244.832	0.510	236.946	0.526	3.221
1000	3	403	851.025	0.149	877.190	0.123	3.075
1000	3	443	729.301	0.271	722.470	0.278	0.937
1000	3	473	505.736	0.494	501.790	0.498	0.786
800	3	403	696.224	0.130	717.110	0.104	2.999
800	3	443	608.664	0.239	635.286	0.206	4.374
800	3	473	440.602	0.449	450.436	0.437	2.232
500	3	403	443.263	0.113	458.840	0.083	3.514
500	3	443	394.000	0.212	414.986	0.170	4.865
500	3	473	295.719	0.409	289.723	0.421	2.027

5.3 Kinetic Analysis of Oxidation Process

The oxidation reaction of the DBT present in LGO using trickle bed reactor tested under various LHSV(1 - 3hr^{-1}), temperature (403 - 473K), initial DBT concentration (500 –1000 ppm), and catalyst (Co_3O_4/γ-Al_2O_3) in order to estimate the reaction kinetics by analyzing the results obtained based on experiments and using kinetic models within gPROMS program. The increase in process conversion happened due to the kinetic factors utilized for describing ODS processes in this model that are affected by the operating conditions. The reaction temperature affects the reaction constants of the ODS operations, where decreasing temperature leads to decrease in the reaction constants according to the Arrhenius equations (and vice versa) so that decreasing temperature decreases the number of molecules involved in the oxidation reaction, which in turn decrease the conversion(and vice versa).

LHSV is also an important operational parameters that estimates the severity of reaction and the efficiency of ODS. With the LHSV decreasing, the reaction rates will be significant. increasing LHSV described by liquid velocity, means decreasing contact time and decreasing conversion of dibenzothiophene.

5.3.1 Activation Energy

Depending on Arrhenius correlation, a plot of (ln*K*) against (1/*T*) will give a straight line with slope equal to (-E_A/R), the activation energy is then evaluated as shown in Figure 6. The generated value of activation energy is introduced to be (35.425 kJ/mole). This value is close to the value obtained by **Sachdeva and Pant.**[39] The low amount of E_A estimated in this work pointed that the oxidation of sulphur is faster in the existence of catalyst. The reaction rate and mathematical kinetic model of dibenzothiophene that can be used with high confidence to reactor design is written as:

❖ **Reaction rate:**

$$-r_{DBT} = \mathbf{18256} * EXP\left(-\frac{4260}{T}\right) * \eta_0 * \eta_{ce} * C_{DBT}^{1.43893} \quad (42)$$

Kinetic models:

$$\frac{X_{DBT}}{1-X_{DBT}} = \frac{18256 \times EXP\left(-\frac{4260}{T}\right) \times \eta_0 \times \eta_{ce} \times 1.43893 \times C_{DBT}{}^{0.43893}}{LHSV} \quad (43)$$

Also, there are many factors affect the activation energy that can be summarized as follows:

❖ Firstly, one of the most important factors is the type of the catalyst. The activation energy of DBT found in the current work is in agreement with that found in the literature, which is 28.48kJ/mole using H_2O_2 and a quaternary ammonium based phosphotungstic acid as the phase transfer catalyst.[40] However, **Ahmed et**

al.[41] reported that the activation energy of DBT is 40.3 kJ/mole using vanadium substituted quaternary ammonium based phosphomolyb-date/H_2O_2/ionic liquid oxidation system.

❖ The second factor affecting the activation energy is the solvent type used, **Ishihara et al.**[42]found that the activation energy of DBT and 4,6 DMDBT in two different types solvent in light gas oil equal to 32 ± 1kJ and 28 ± 1kJ in kerosene.

❖ The third factor is the type of the sulphur compound, which is individual. Such that activation energies for sulfur removal was evaluated to be 65.3 kJ/mole for DBT and 61.9 kJ/mole for BT, respectively. [43]The E_A of ODS for (DBT, 4-MDBT) and (4,6-DMDBT) was reported to be almost the same with a mean value of (29.1 kJ/mole) and for BT equal to 34.6 kJ/mol. The variation between the E_A of BT and that of DBTs can be attributed to the electron density values on sulphur atom for BT, which is remarkably lower than that of DBTs. [5]

5.4 Effectiveness Factor

The influence of Thiele modulus, and Effectiveness Factor on catalyst activity, are illustrated in Figures 7a, b, c. Thiele modulus and effectiveness factor is calculated according to the mathematical modeling introduced in this study within gPROMS. The following observations are made: decreasing of DBT concentration decreases Thiele modulus values slightly because it affects the values of the reaction constant as stated in Figure 7a. Therefore, the decrease of DBT concentrations increase the effectiveness factor as illustrated in Figure7b.

It is noticed from Figure 7b that the Thiele modulus and Effectiveness factor have explained why Co_3O_4/γ-Al_2O_3 is the best catalyst due to the low values of Thiele modulus and high values of Effectiveness factor.

It has been noted that the effectiveness factor increases with decreasing reaction temperature and LHSV. When temperature is decreased, a more stronger decrease in the reaction constant is obtained than diffusivity. This will lead to a more pronounced diffusion limitation since it becomes the limiting step and thus to smaller effectiveness factors. When LHSV is decreased at fixed temperature, the increase in the effectiveness factor can be reported to the decreased reaction mixture viscosity, which is got at lower LHSV, since viscosity is directly related with reactants diffusivity and a decrease in viscosity will lead to an increase in effectiveness factor. [44]These results agree with Figures 7b and 7c obtained from present study.

5.5 The Influence of Oxidation Process on Physical Properties of Light Gas Oil

The physical properties and ASTM distillation of feedstock and product at optimum operating condition (temperature =473K, *LHSV* =1hr $^{-1}$, dibenzothiophene initial concentration =1000 ppm) are illustrated in Table 7 and Table 8. It is obvious that there is no high difference in physical properties and ASTM distillation between feedstock and product at the optimum operating condition. This attributes to the following reasons:-

- Density, viscosity, and boiling range are approximately the same before and after oxidation reaction because there was no high change in the components of hydro treated light gas oil.

- Reid vapor pressure (RVP) decrease slightly because some of volatile compounds are reacted

- Aniline points (AN) and research octane number (RON) are the same before and after oxidation reaction approximately, due to the aromatic compounds not involved in the oxidation reaction , so that they are not break or saturated as in hydrodesulphurization process.

Table 7: Some physical properties of feedstock *(light gas oil)* before oxidation and after oxidation at (*LHSV*=1hr^{-1}, T=473K and I.C=1000 ppm).

Specification	LGO Before ODS	LGO after ODS at optimum condition
RVP psig (312 K)	16.3	15.8
Viscosity cst (293 K)	4.9	4.7
Density (gm/cm^3)	0.8423	0.851
°API	36.4	34.8
Boiling range (K)	333-485	322-545
AP (K)	412	416
RON	87	83

Table 8: ASTM distillation of feedstock *(light gas oil)* before oxidation and after oxidation at (*LHSV*=1hr^{-1}, T=473K and I.C=1000 ppm).

Distillate volume	Light gas oil before ODS (K)	Light gas oil after ODS at optimum condition (K)
Initial	433	447
10 %	481	487
20 %	499	504
30 %	514	523
40 %	531	538
50 %	545	557
60 %	563	569
70 %	581	587
80 %	599	604
90 %	624	630
Final	633	643
Distillate %	97.5 %	98%
Loss	2.5 %	2 %

6. Conclusions

1. A model sulphur compound has investigated here to estimate the effectiveness of oxidative desulfurization operation as well as test the kinetics model of the oxidation reaction based on experiments. Generally, the oxidation of organic sulphur components under oxidative desulfurization conditions follow (1.439) order kinetic for $Co_3O_4/\gamma\text{-}Al_2O_3$ catalyst. The optimal apparent rates constant of dibenzothiophene in LGO are found to be 2.48282 ($hr^{-1} * (Wt)^{-0.43893}$) at 473K for DBT. This information is very significant to design a continuous oxidative desulfurization system and the process estimation of oxidative desulfurization for LGO.
2. Optimization problem has formulated for optimizing the design and operation condition base on minimizing an objective function involving design and operating parameters.
3. Oxidation reaction simulated based on the kinetic parameters estimated from previous works gives large error percent between predicted and experimental compositions of fractions. Therefore, the optimization technique has been applied to obtain the best kinetic model depending on the experimental. The results of application of optimal kinetic parameters in simulation gives good agreement between predicted and experimental compositions with absolute less than 5% among all result and the model can now be confidently used to reactor design, operating and control, and also for predicting the concentration profiles of any component at any conditions.

Nomenclature

$\Delta\rho_p$	Pressure dependence of liquid density	lb/ft^3
$\Delta\rho_T$	Temperature correction of liquid density	lb/ft^3
C_{DBT}	Concentration of dibenzothiophene	cm^3/mole
C_{in}	Initial concentration (inlet to reactor)	cm^3/mole
C_{out}	Final concentration (outlet from reactor)	cm^3/mole
D_{Ki}	Knudsen diffusivity factor	cm^2/sec
D_{ei}	Effective diffusivity	cm^2/sec
D_{mi}	Molecular diffusivity	cm^2/sec
d_p	Particle diameter	cm
d_{pe}	Equivalent particle diameter	cm
d_t	Tube diameter	cm
K_o	Frequency or pre-exponential factor	cm^3/g. sec
K_{app}	Apparent reaction rate constant	-
K_{in}	Kinetic rate constant	$(time)^{-1}(con.)^{1-n}$
MW_i	Molecular weight of oxygen	g/gmole
Mw_L	Molecular weight of liquid phase	g/gmol
r_{DBT}	Dibenzothiophene rate of reaction	
r_g	Mean pore radius	cm
r_p	Radius of particle	cm
S_g	Specific surface area of particle	cm^2/g
S_P	External surface area of catalyst particle	cm^2
$Sp.gr_{15.6\backslash}$	Specific gravity of oil at 15.6 ^oC	-
T_{meABP}	Mean average boiling point	R
u_L	Velocity of the liquid	cm/sec
V_{CDBT}	Critical specific volume of the DBT compound	ft^3/mole
V_{CL}	Critical specific volume of liquid	cm^3/mole
V_{DBT}	Molar volume of DBT at n.b. temperature	cm^3/mole

V_g	Total pore volume	cm^3/g
V_L	Molar volume of liquid at its n.b. temperature	cm^3/mole
V_P	Volume of catalyst particle	cm^3
μ_L	Dynamic viscosity of liquid phase	mPas. sec
$\rho_{15.6}$	Density of light gas oil at 15.6 ^oC	g/cm^3
ρ_B	Bulk density	g/cm^3
ρ_L	Liquid density at process condition	lb/ft^3
ρ_o	Density of light gas oil at 15.6 ^oC and 101.3 Kpa	lb/ft^3
ρ_p	Particle density	g/cm^3
A	Dimensionless number	-
EA	Activation energy	kJ/mole
F_{DBT}	Input of dibenzothiophene	moles/time
g	Acceleration	cm/sec^2
K	Reaction rate constant	$hr^{-1}.wt^{(n-1)}$
n	Order of reaction kinetic	-
ppm	Part per million	-
R	Universal gas constant	8.314 J/mol. K
T	Temperature	K or ^oC
V	Bed volume of particle catalyst	cm^3
V_L	Volumetric flow of liquid phase	cm^3/time
V_P	Pore volume	cm^3
τ	Residence time	hr

Greek letters

465

η_{ce}	External catalyst wetting efficiency
ϵ_S	Catalyst porosity
$\mathcal{T}$	Tortuosity factor
Φ	Thiele modulus
ϵ_B	Bed void fraction

References

[1] Mei, H.;Mei, B.W.; Yen, T.F. A new method for obtaining ultra-low sulphur diesel fuel via ultrasound assisted oxidative desulphurization. *Fuel* ***2003****, 82, 405–414*.

[2] Schmitz, C.; Datsevitch, L.; Jess, A. Deep desulphurization of diesel oil: kinetic studies and process-improvement by the use of a two-phase reactor with pre-saturator. *Chem. Eng. Sci.* ***2004****, 59, 2821–2829*.

[3] Tailleur, R.G.; Ravigli, J.; Quenza, S.; Valencia, N. Catalyst for ultra-low sulphur and aromatic diesel. *Appl. Catal. A Gen.* ***2005****, 282, 227–235*.

[4] Zannikos, F.; Vignier, V. Desulphurization of petroleum fractions by oxidation and solvent extraction. *Fuel Processing Technology* ***1995****, 42,35–45*.

[5] Otsuki, S.; Nonaka, T.; Takeshi, N.; Takashima, N.; Qian, W.; Ishihara, A.; Imai, T.; Kabe, T. Oxidative desulphurization of light gas oil and vacuum gas oil by oxidation and solvent extraction. *Energy & Fuels* ***2000****, 14, 1232–1239*.

[6] Wang, D.; Qian, E.W.; Amano, H.; Okata, K.; Ishihara, A.; Kabe, T. Oxidative desulphurization of fuel oil, Part I. Oxidation of dibenzothiophene using *tert-butyl* hydroperoxide. *Appl. Catal. A Gen.* ***2003****, 253, 91–99*.

[7] Chica, A.; Corma, A.; Domine, M.E. Catalytic oxidative desulphurization (ODS) of diesel fuel on a continuous fixed-bed reactor. *J. Catal.* ***2006****, 242,299–308*.

[8] Chica, A.; Gatti, G.; Moden, B.; Marchese, L.; Iglesia, E. Selective catalytic oxidation of organ sulphur compounds with *tert-butyl* hydroperoxide. *Chem. Eur. J.* ***2006****, 12, 1960–1967*.

[9] Ali, M.F.; Al-Malki, A.; El-Ali, B.; Martinie, G.; Siddiqui, M.N. Deep desulphurization of gasoline and diesel fuels using non-hydrogen consuming techniques. *Fuel* ***2006****, 85, 1354–1363*.

[10] Babich , I.V.; Moulijn, J.A. Science and technology of novel processes for deep desulphurization of oil refinery streams: a review. *Fuel* ***2003***, 82 , pp. 607–631.

[11] Zaho, D.; Sun, F.; Zhou, E.; Liu Y. A review of desulphurization of light oil based on selective oxidation. *Chemical journal on internet* ***200 6***, pp. 17-20.

[12] Long, R.B.; Caruso, F.A. Selective separation of heavy oil using a mixture of polar and nonpolar solvents. U.S. *Patents* ***1985***, 4, 493, 756.

[13] Gore, W. Method of desulphurization of hydrocarbons. USA *Patents* ***2001***, 6, 274-785.

[14] Mei, H.; Mei, B.W.; Yen, F.T. A new method for obtaining ultralow sulphur diesel fuel via ultrasound assisted oxidative desulphurization, *Fuel*, ***2003***, 82, 405- 414.

[15] Attar, A.; Corcon, W.H. Desulphurization of organic compounds by selective oxidation. *Ind. Eng. Chem*., ***1978***, 17, 102-109.

[16] Aida, T. Method of recovering organic sulphur compounds from liquid fuel. European. *Patent*, ***1993***,656, 324.

[17] Ma, X.; Zhou, A.; Song, S. A novel method for oxidative desulphurization of liquid hydrocarbon fuels based on catalytic oxidation using molecular oxygen coupled with selective adsorption. *Catalysis Today*, ***2007***,123, 276–284.

[18] Murata, S.; Murata, K.; Kidena, K.; Nomura, M. A. Novel Oxidative Desulphurization System for Diesel Fuels with Molecular Oxygen in the Presence of Cobalt Catalysts and Aldehydes. Energy & Fuels ***2004***, 18 , 116.

[19] Ancheyta, J.;Speight J.G. Hydroprocessing of Heavy Oils and Residua; Taylor & Francis: New York: CRC Press, ***2007***.

[20] Ancheyta, J. Modeling and Simulation of Catalytic Reactors for Petroleum Refining, John Wiley & Sons: New Jersey, ***2011***.

[21] gPROMS. Introductory user guide, Process System Enterprise Ltd (PSE),***2005***. http:// www.psenterprise.com/gproms/.

[22] Bej, S.K.; Dalai, A.K.; Adjaye, J. Comparison of hydrodenitrogenation of basic and non-basic nitrogen compounds present in oil sands derived heavy gas oil. *Energy & Fuels* ***2001***, *15,377-383*.

[23] Khalfhallah, H.A. Modelling and optimization of oxidative desulphurization process for model sulphur compounds and heavy gas oil. PhD Thesis, UK, University of Bradford, ***2009***.

[24] Macı´as, M.J.; Ancheyta, J. Simulation of an isothermal hydrodesulphurization small reactor with different catalyst particle shapes. *Catal. Today* ***2004***, *98, 243-252*.

[25] Alvarez, A.; Ancheyta, J. Modeling residue hydroprocessing in a multi-fixed-bed reactor system. *Applied Catalysis A: General* ***2008***, *351,148-158*.

[26] Pitault, I.; Fongarl, P.; Mitrovic, M.; Ronze, D.; Forissier, M. Choiceof Laboratory Scale Reactors for HDT Kinetic Studies or Catalyst Tests. *Catal. Today* ***2004***, *98,31–42*.

[27] Al-Dahhan, M.H. Recent Advances and Scale-up of Trickle Bed Reactors for Energy and Environmental Applications, Proceedings – International Symposium on Advances in Hydro processing of Oil Fractions, Morelia, Mexico, June ***2007***, 26-29.

[28] Froment, G.F.; Bischoff, K.B. Chemical Reactor Analysis and Design, John Wiley and Sons Inc: New York: ***1990***.

[29] Jarullah, A.T.; Iqbal, M.M.; Wood, A.S. Kinetic model development and simulation of simultaneous hydrodenitrogenation and hydrodemetallization of crude oil in trickle bed reactor. *Fuel **2011**, 90, 2165–2181*.

[30] Mederos, F.S.; Elizaldi, G.; Ancheyta, J. Steady-State and Dynamic Reactor Models for Hydrotreatment of Oil Fractions: A Review. *Catalysis Review **2009**, 51, 485-607*.

[31] Mederos, F.S.; Rodrı´guez, M.A.; Ancheyta, J.; Arce, E.Dynamic Modelling and Simulation of Catalytic Hydrotreating Reactors. *Energy & Fuels **2006**, 20, 936-945*.

[32] Jarullah, A.T.; Iqbal, M.M.; Wood, A.S.Kinetic parameterestimation and simulation of trickle-bed reactor for hydrodesulphurization of crude oil. *Chemical Engineering Science **2010**, 66, 859–871*.

[33] Ahmed T. Hydrocarbon Phase Behavior.Houston: Gulf Publishing: 1989.

[34] Al-Dahhan, M.H.; Dudukovic, M.P. Catalyst Wetting Efficiency in Trickle-Bed Reactors at High-Pressure. *Chem. Eng. Sci. **1995**, 50, 2377-2389*.

[35] Jarullah, A.T.; Iqbal, M.M.; Wood, A.S. Improving fuel quality by whole crude oil hydrotreating: A kinetic model for hydrodeasphaltenization in a trickle bed reactor. *Applied Energy **2012**, 94,182–191*.

[36] Jimenez, F.; Nunez, M.; Kafarov, V. Modeling of industrial reactor for hydrotreating of vacuum gas oils Simultaneous hydrodesulphurization, hydrodenitrogenation and hydrodearomatization reactions. *Chemical Engineering Journal **2007**, 134, 200-208*.

[37] Poyton, A. A.; Varziri, M.S.; McAuley, K.B.; McLellan, P.J.; Ramsay, J.O. Parameter estimation in continuous-time dynamic models using principal differential analysis. *Comput. Chem. Eng. **2006**, 30, 698–708*.

[38] Nawaf, A. T., Gheni, S. A; Jarullah, A.T.; Mujtaba, I.M. Optimal Design of a Trickle Bed Reactor for Light Fuel Oxidative Desulphurization based on Experiments and Modeling. *Energy & Fuels **2015**,29, 3366-3376*.

[39] Sachdeva, T.O.; Pant, K.K. Deep desulphurization of diesel via peroxide oxidation using phosphotungstic acid as phase transfer catalyst. *Fuel Processing Technology **2010**, 91, 1133-1138*.

[40] Huang, D.; Lu, Y.C.; Wang, Y.J.; Luo, G.S. Catalytic Kinetics of Dibenzothiophene Oxidation with the Combined Catalyst of Quaternary Ammonium Bromide and Phosphotungstic. Acid. *Ind. Eng. Chem. Res.* ***2007****, 46, 6221-6227.*

[41] Ahmad, I.; Ahmad, W.; Ishaq, M. Desulphurization of liquid fuels using air-assisted performic acid oxidation and emulsion catalyst. *Chinese Journal of Catalysis* ***2013****, 34, 1839-1847.*

[42] Ishihara, A.; Wang, D.; Dumeignil, F.; Amano, H.; Qian, E.W.; Kabe, T. Oxidative desulphurization and denitrogenation of a light gas oil using an oxidation/adsorption continuous flow process. *Applied Catalysis A: General* ***2005****, 279, 279–287.*

[43] Shiraishi, Y.;Tachibana, K.; Hirai, T.; Komasawa , I. Desulphurization and denitrogenation Process for Light Oils Based on Chemical Oxidation followed by Liquid-Liquid Extraction. *Ind. Eng. Chem. Res.* ***2002****, 41, 4362-4375.*

[44] Martnez, J.;Ancheyta, J. Kinetic model for hydrocracking of heavy oil in a CSTR involving short term 3 catalyst deactivation. *Fuel* ***2012****,100,193-199.*

List of Figures

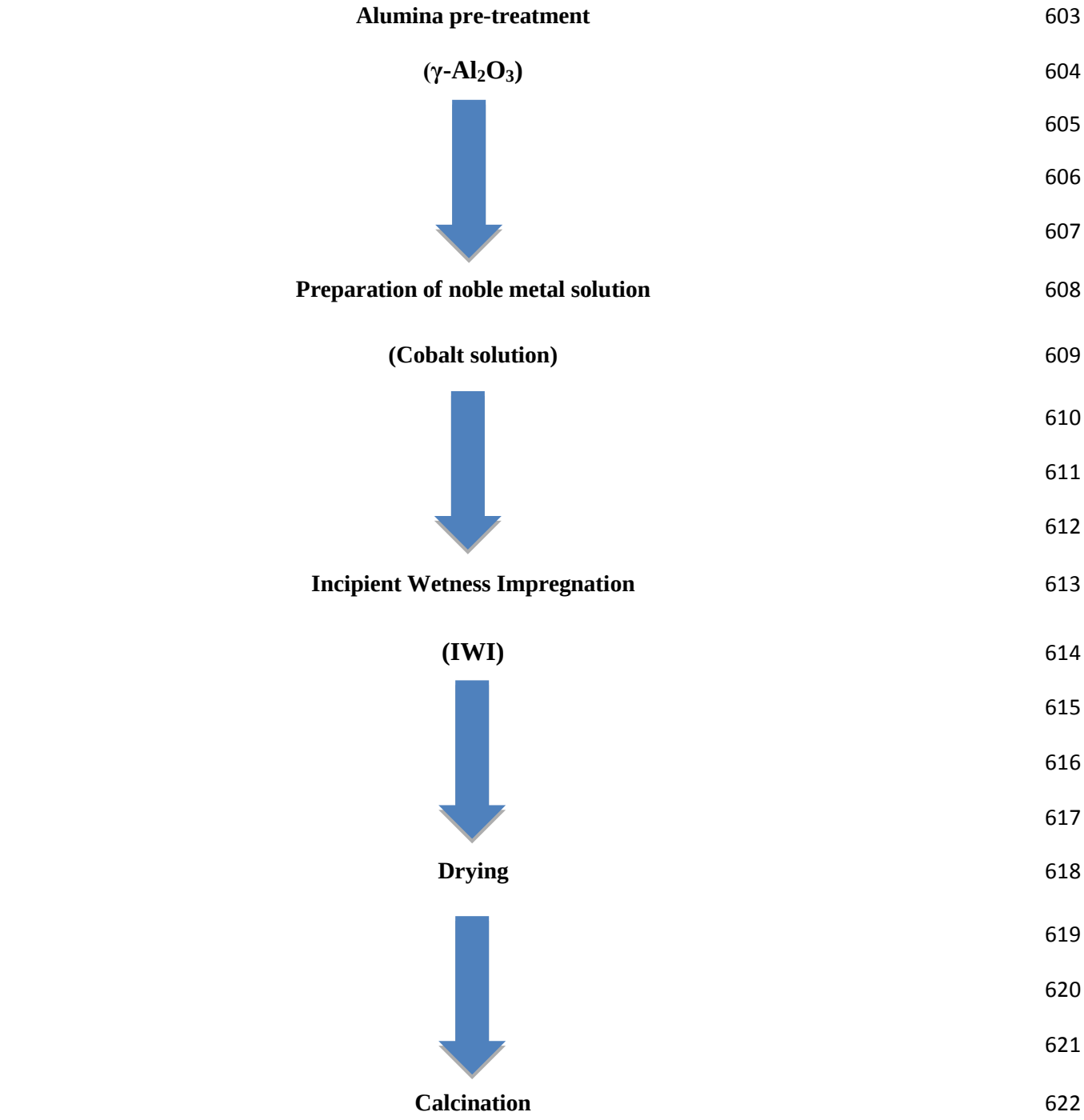
Alumina pre-treatment
(γ-Al2O3)
Preparation of noble metal solution
(Cobalt solution)
Incipient Wetness Impregnation
(IWI)
Drying
Calcination

Figure 1

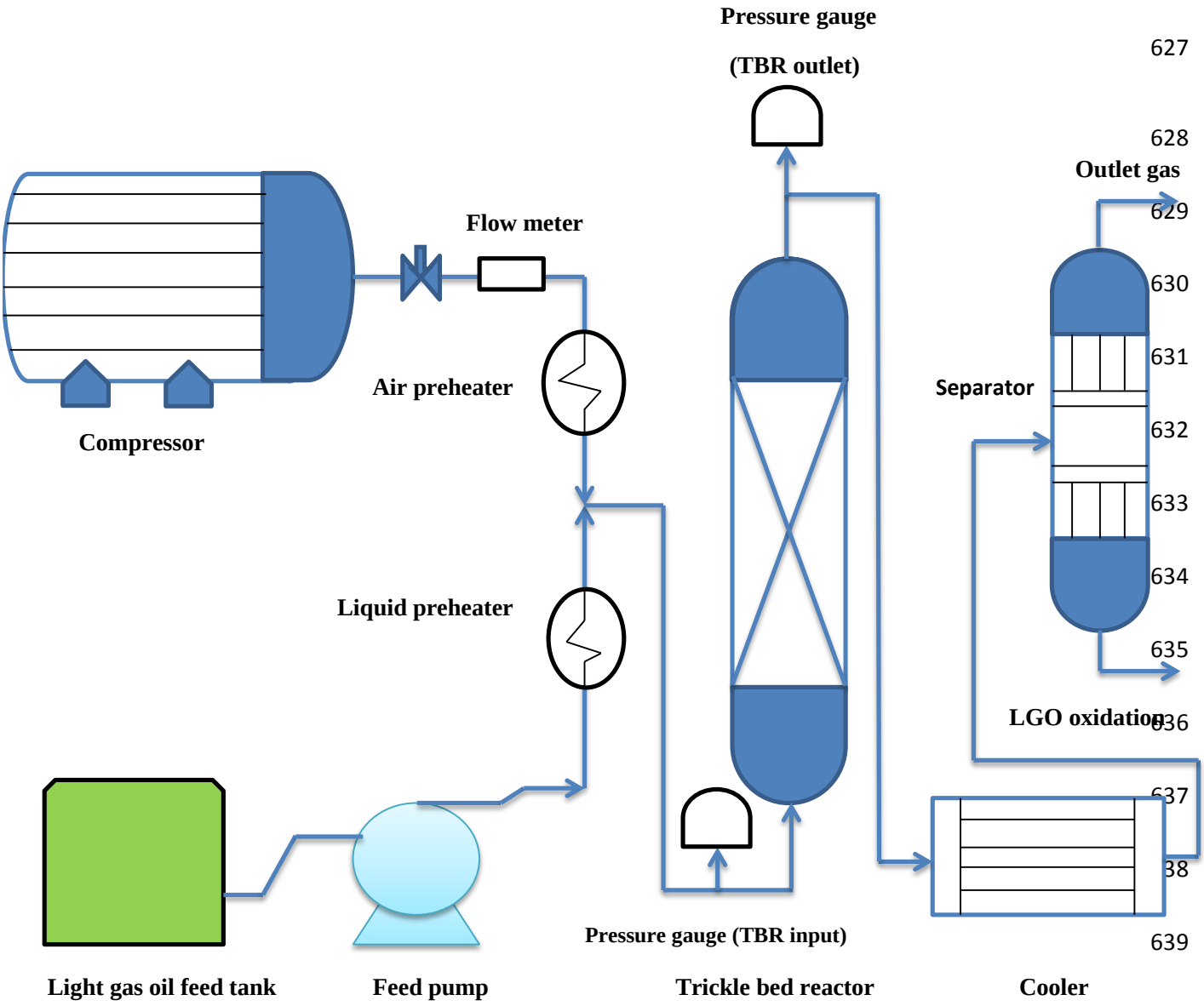
Pressure gauge
(TBR outlet)
Outlet gas
Flow meter
Separator
Air preheater
Compressor
Liquid preheater
LGO oxidation
Light gas oil feed tank
Feed pump
Pressure gauge (TBR input)
Trickle bed reactor
Cooler

Figure 2

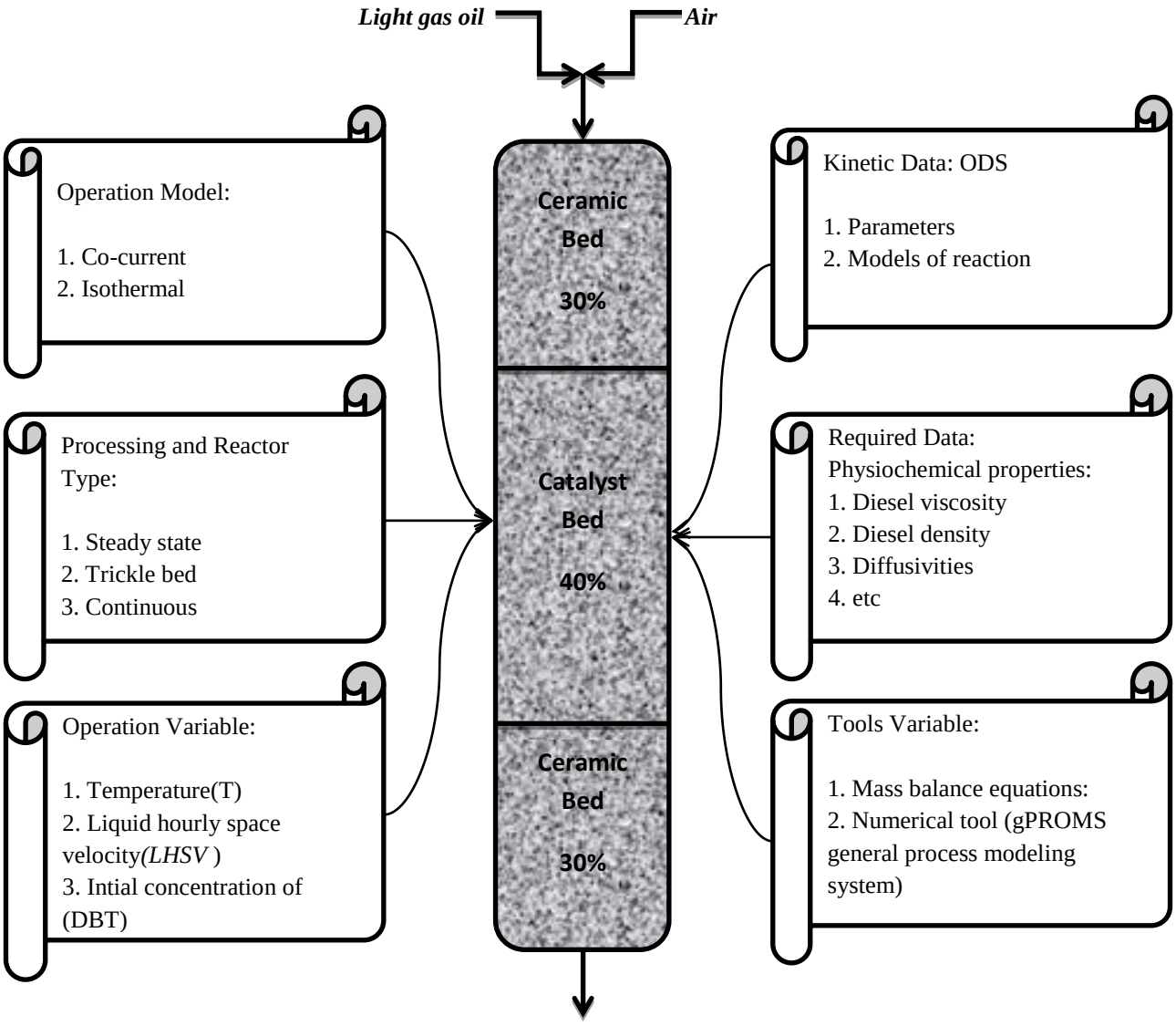

Light Gas Oil Desulphurization

Figure 3

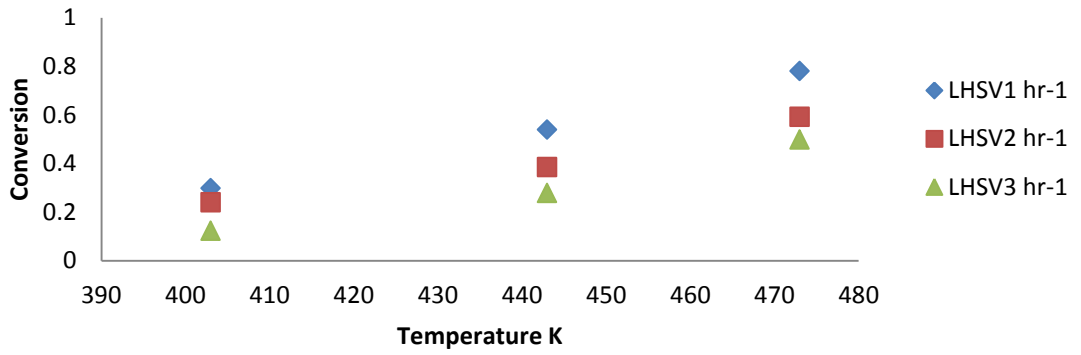

673

(a)

674

675

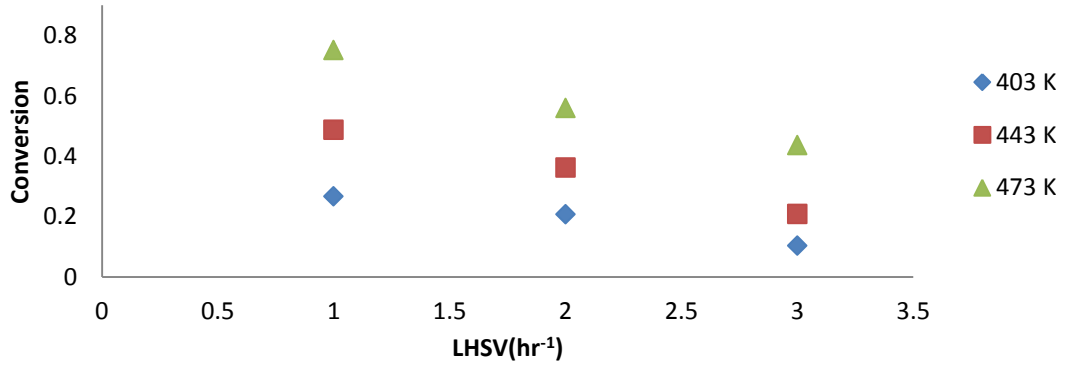

676

(b)

677

678

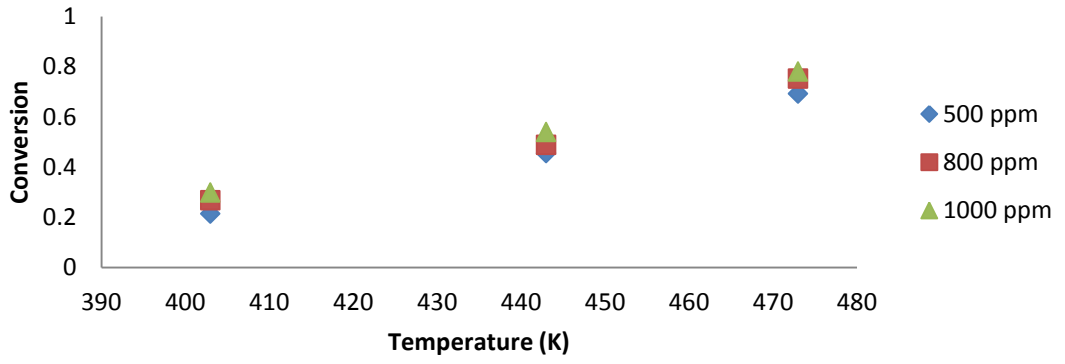

679

(c)

680

681

Figure 4

682

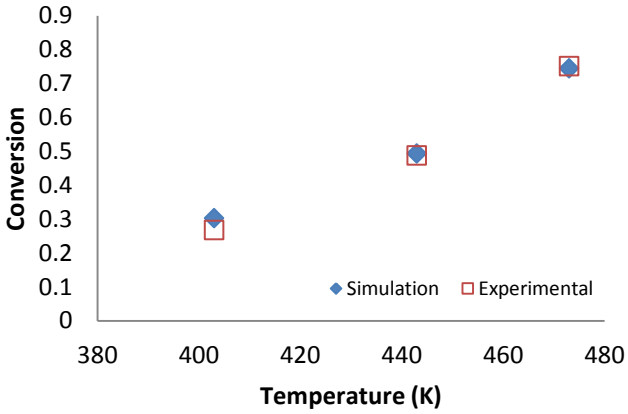

(a)

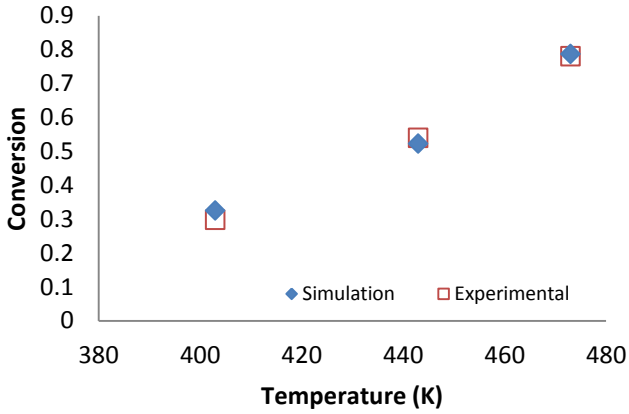

(b)

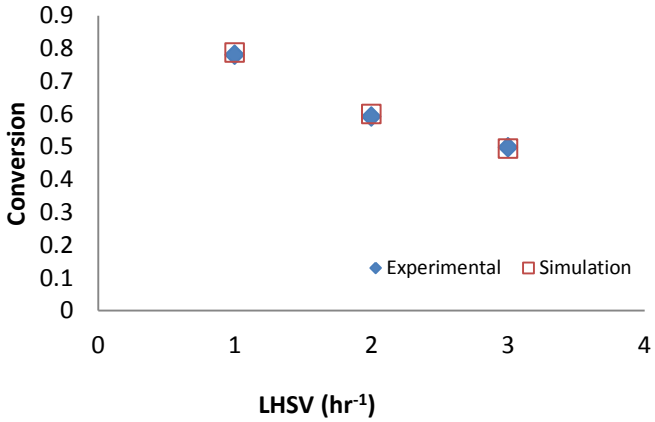

(b)

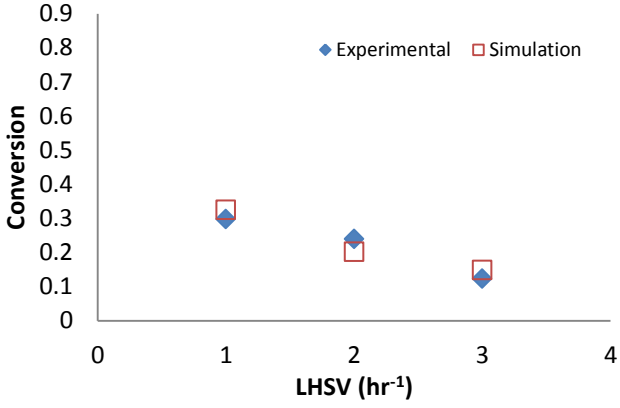

(d)

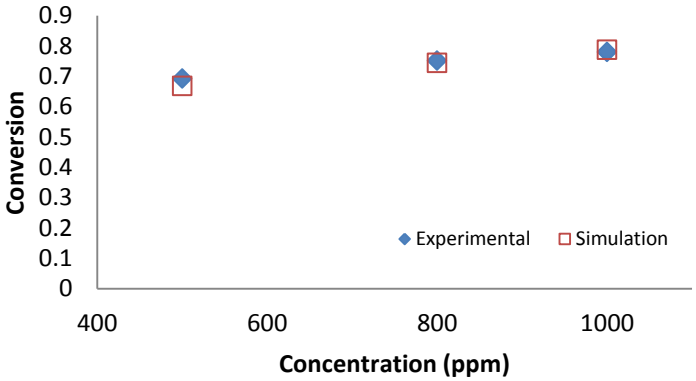

(e)

Figure 5

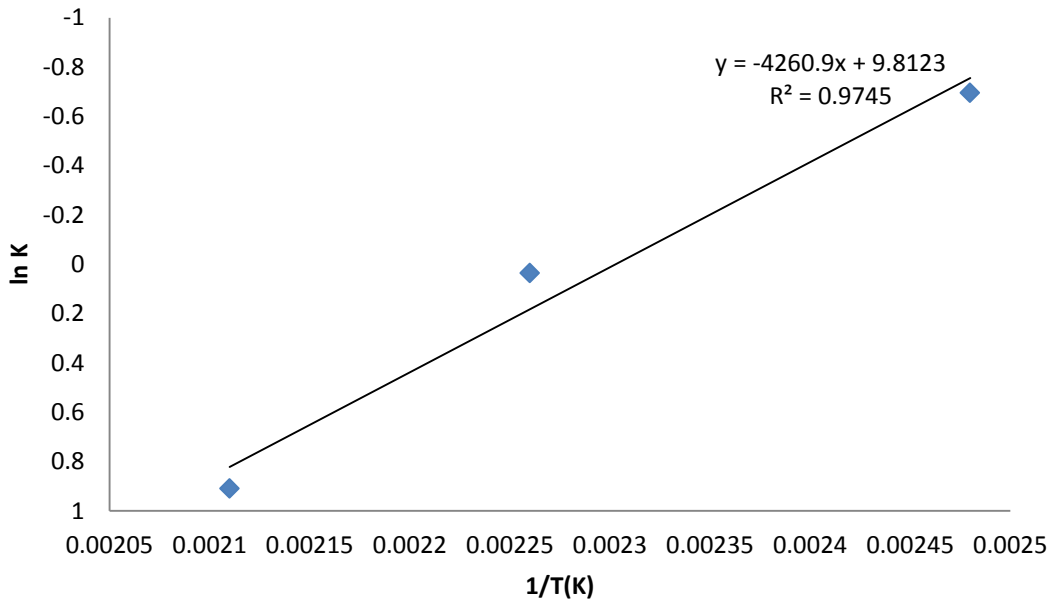

690

691

692

693

694

695

696

697

698

699

700

701

702

Figure 6

703

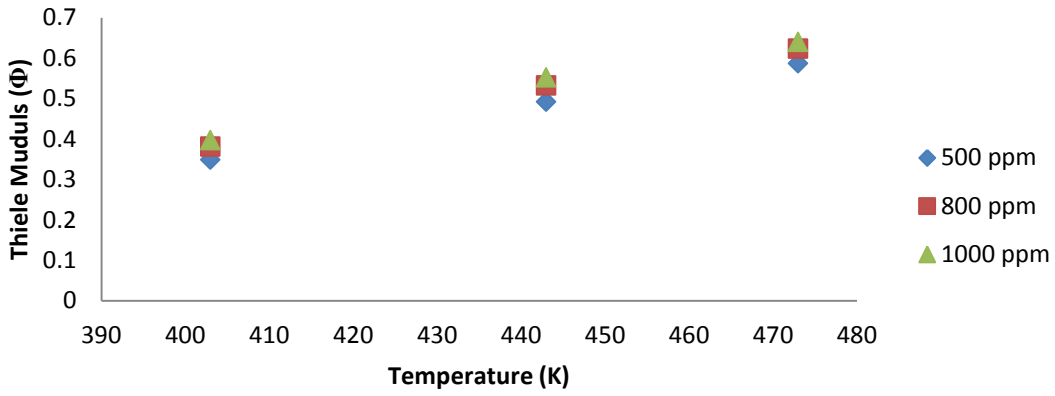

704

(a)

705

706

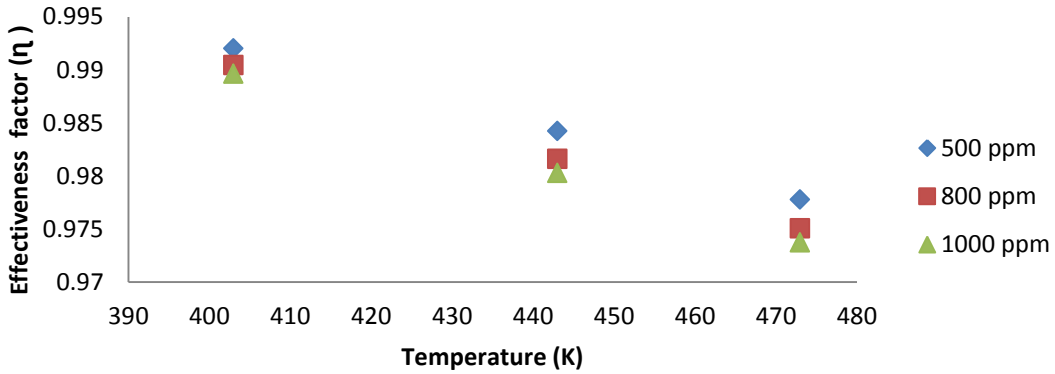

707

(b)

708

709

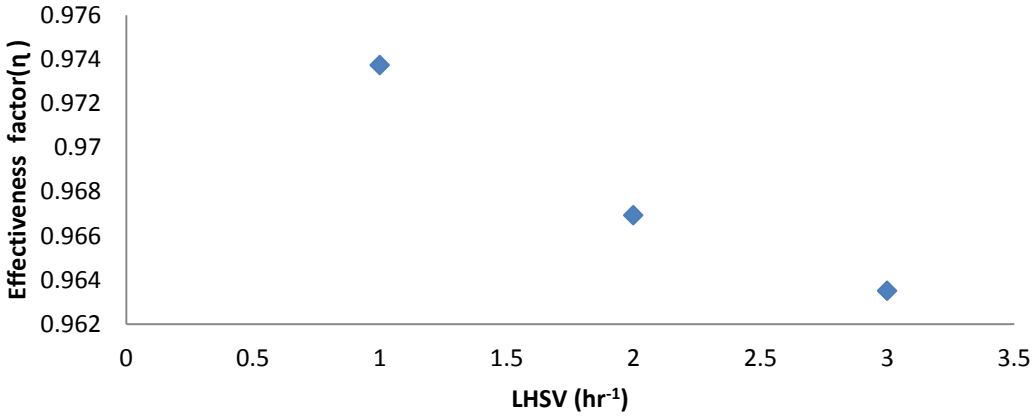

710

(c)

711

Figure 7

712